Chemistry
A European
Journal

Chemistry Europe
European Chemical Societies Publishing

Accepted Article

Title: [Gd(AAZTA)]- derivatives with n-alkyl acid side chains show improved properties for their application as MRI contrast agents

Authors: Zsolt Baranyai, Flávio Vinicius Crizóstomo Kock, Attila Forgács, Nicol Guidolin, Rachele Stefania, Adrienn Vágner, Eliana Gianolio, and Silvio Aime

To be cited as: *Chem. Eur. J.* 10.1002/chem.202004479

Link to VoR: https://doi.org/10.1002/chem.202004479

WILEY-VCH

10.1002/chem.202004479

WILEY-VCH

[Gd(AAZTA)]$^-$ derivatives with *n*-alkyl acid side chains show improved properties for their application as MRI contrast agents

Flávio Vinicius Crizóstomo Kock,[a,b] Attila Forgács,[c,d] Nicol Guidolin,[e] Rachele Stefania,[b] Adrienn Vágner,[c] Eliana Gianolio,*[b] Silvio Aime[b] and Zsolt Baranyai*[e]

Abstract: Herein the synthesis and an extensive characterization of two novel Gd(AAZTA) derivatives functionalized with short (C_2 and C_4) *n*-alkyl acid function are reported. The carboxylate functionality is the site for further conjugations for the design of more specific contrast agents (CAs). Interestingly it has been found that the synthetized complexes display enhanced properties for their use as MRI contrast agents by their own. The stability constants determined using potentiometric titration and UV-Vis spectrophotometry were slightly higher than the one reported for the parent Gd(AAZTA) complex. This observation might be accounted in terms of the larger sigma-electron donation of the acyl substituents in respect to the one provided by the methyl group in the parent complex. As far as concerns the kinetic stability, transmetallation experiments with endogenous ions (e.g. Cu^{2+}, Zn^{2+} and Ca^{2+}) led to infer that the Gd^{3+} ions present in these Gd(AAZTA) derivatives show somewhat smaller susceptibility to chemical exchange towards these ions at 25°C, close to the physiological condition. The ^{1}H-NMR spectra of the complexes with Eu^{III} and Yb^{III} displayed a set of signals consistent with half the number of methylene protons present on each ligand. The number of resonances resulted invariant over a large range of temperature to suggest the occurrence of a fast interconversion between structural isomers. The relaxivity values (298K, 20MHz) were consistent with q=2 being equal to 8.8 $mM^{-1}.s^{-1}$ for the C_2 derivative and 9.4 $mM^{-1}s^{-1}$ for the C_4 one, i.e sensibly larger than the one reported for Gd(AAZTA) (7.1 $mM^{-1}.s^{-1}$). VT-T_2 ^{17}O-NMR measurements showed, for both complexes, the presence of two populations of coordinated water molecules, one in fast and one in slow exchange with the bulk water. Since the high resolution ^{1}H-NMR spectra of the analogues with Eu(III) and Yb(III) did not show the occurrence of distinct isomers (as frequently observed in other macrocyclic Lanthanide(III)-containing complexes), we surmised the presence of two fast-interconverting isomers in solution. The analysis of the ^{17}O NMR VT-T_2 profiles vs. temperature allowed to establish their relative molar fraction being 35% for the isomer with the fast exchanging water and 65% for the isomer with the water molecules in slower exchange. Finally, ^{1}H NMRD profiles over an extended range of applied magnetic field strengths have been satisfactory fitted on the basis of the occurrence of the two interconverting species.

Introduction

The design of novel contrast agents (CAs) for magnetic resonance imaging (MRI) is still a task of strong interest in the search of safe, rapid and non-invasive clinical diagnostics.[1] Up to now these CAs are represented by paramagnetic metal complexes characterized by a high longitudinal paramagnetic relaxivity (r_{1p}). Several paramagnetic ions, among them Mn^{2+}, Mn^{3+}, Fe^{3+}, and Gd^{3+} can exerts a strong paramagnetic effect on the water proton relaxation being Gd^{3+} ions the candidate of choice due to the high paramagnetism associated to its seven unpaired electrons and the relatively long electron relaxation time.[2–4]

It was immediately evident, in the early days of their suggestion as MRI-CAs, that free Gd^{3+} ions could not be administered to living systems because of their antagonistic role in respect to the endogenous Ca^{2+} and Zn^{2+} ions .[3] Therefore, the complexation of Gd^{3+} ions with ligands to yield highly stable chelates has been a fundamental step in the search of new contrast agents. Nowadays, the clinically used Gd^{3+}-based contrast agents (GBCAs)[5] own only one water molecule coordinated (q=1) to the paramagnetic ion,[6] in spite of the fact that the relaxivity scales up with the number of coordinated water molecules. This choice relies on the early observation that the coordination with octa-dentate ligands yields highly stable complexes which ensure for a limited *in vivo* release of Gd^{3+} ions. However, the search for systems containing two or three coordinated water molecules still endowed with a stability compatible with their *in vivo* use, is an area of intense activity.[7,8] In this context, the AAZTA ligand (6-amino-6-methylperhydro-1,4-diazepine tetra acetic acid) (and its derivatives) has been considered as an excellent system for the design of q=2 GBCAs (Scheme 1). In fact high relaxivities were reported for AAZTA chelates forming lipid-based aggregates [9] or able to bind to human serum albumin (HSA)[10] . For these applications bifunctional AAZTA derivatives were designed to embody remote free functional groups ready for the conjugation step with the selected moieties.[11–15] The aim of the herein reported work was to address a detailed physico-chemical characterization of two novel Gd(AAZTA) derivatives functionalized with short (C_2 and C_4) spaced acid function (Scheme 1), designed for being used in further conjugations with a variety of targeting vectors, lipophilic chains or to form multimeric species.

[a] F. V. C. Kock, São Carlos Institute of Chemistry, University of São Paulo, Avenida Trabalhador São Carlense 400, 13566-590, São Paulo, Brazil
[b] F. V. C. Kock, Dr. E. Gianolio, R. Stefania, Prof. S. Aime, Dep. of Molecular Biotechnologies and Health Science, University of Turin, Via Nizza 52, 10125, Turin, Italy. E-mail: eliana.gianolio@unito.it
[c] Dr. A. Forgács, Dr. A. Vágner, Dep. of Inorganic and Analytical Chemistry, University of Debrecen, H-4010, Debrecen, Egyetem tér 1., Hungary
[d] Dr. A. Forgács, MTA-DE Redox and Homogeneous Catalytic Reaction Mechanisms Research Group, Egyetem tér 1, Debrecen, H-4032 Hungary
[e] N. Guidolin, Dr. Zs. Baranyai, Bracco Imaging SpA, Bracco Research Center, Via Ribes 5, 10010, Colleretto Giacosa (TO), Italy. E-mail: zsolt.baranyai@bracco.com

Supporting information for this article is given via a link at the end of the document. Experimental details of the thermodynamic, kinetic and relaxometric studies; VT-^{1}H NMR spectra of Eu(III) and Yb(III)-complexes

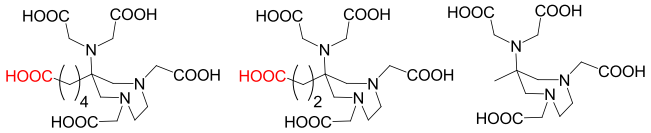

H_4AAZTA-C4-COOH **H_4AAZTA-C2-COOH** **H_4AAZTA**

Scheme 1. Structure of H_4AAZTA, H_4AAZTA-C2-COOH and H_4AAZTA-C4-COOH ligands

Results and Discussion

The H_4AAZTA-C2-COOH and H_4AAZTA-C4-COOH ligands are the derivative of H_4AAZTA in which the methyl group is substituted by *n*-propionic and *n*-valeric acid pendants (Scheme 1) for conjugation purposes.[15,16] Generally three N- and four carboxylate O-atoms can simultaneously bind the metal ion in the AAZTA-complexes.[17–22] The presence of *n*-propionate and *n*-valerate pendants instead of the methyl substituent might affect the equilibrium, kinetic, relaxation and structural properties of the metal complexes formed with AAZTA-C2-COO^- and AAZTA-C4-COO^- ligands. Indeed, the presence of the n-valeric acid pendant used for the conjugation of DATA ligand (DATA^{5m}) to biologically active molecules evidently influence the physico-chemical properties of the Ga^{III}-complexes.[13–15] In order to get more insights into the role the conjugating moieties may have on the physico-chemical properties, the behaviour of the metal complexes formed with the AAZTA-C2-COO^- and AAZTA-C4-COO^- has been investigated close to physiological condition (0.15 M NaCl, 25°C).

Synthesis of ligands and their Ln^{III}-complexes (Ln = Gd^{3+} and Eu $^{3+}$)

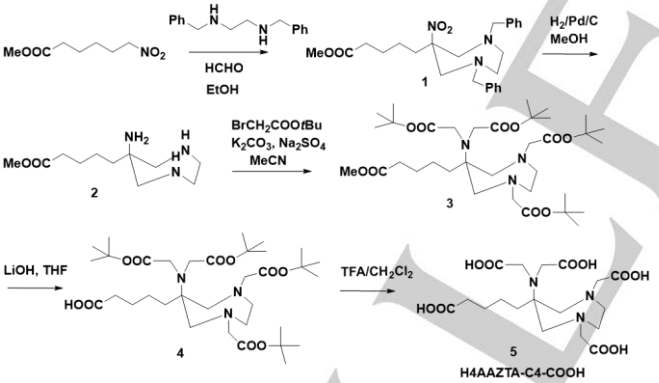

Scheme 2. The synthesis of H_4AAZTA-C4-COOH

The synthesis route of the ligand H_4AAZTA-C4-COOH (**5**) is shown in Scheme 2. It was obtained from its bifunctional prochelating agent AAZTA-C4-(*t*Bu)$_4$ (**4**) after cleavage of all protective groups with trifluoroacetic acid (TFA). Compound **4** was successfully synthesized over 4-steps following the protocol described by Manzoni et al. [12] Briefly, compound **1**, a diazepane ring, was formed via a double nitro-Mannich reaction between *N*,*N*′-dibenzylethylenediamine, paraformaldehyde and 6-nitrohexanoic acid methyl ester in nearly quantitative yield. Hydrogenolysis using palladium on carbon and H_2 removed the benzyl protecting groups at the endocyclic amines and simultaneously reduced the nitro group to an amine. The product was directly reacted with *tert*-butyl bromoacetate to form tetra alkylated compound **3**. Deprotection of the methyl ester protecting groups were carried out by using 1 M lithium hydroxide and tetrahydrofuran (THF) solution to receive the bifunctional chelator AAZTA-C4-(tBu)$_4$.

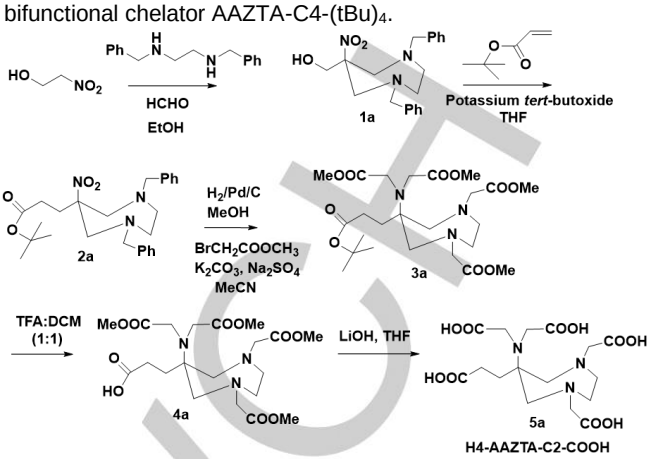

Scheme 3. The synthesis of H_4AAZTA-C2-COOH

The synthesis route of the ligand H_4AAZTA-C2-COOH (**5a**) is shown in Scheme 3, it was obtained from its bifunctional prochelating agent AAZTA-C2-(Me)$_4$ (**4a**) by ester hydrolysis of all protective groups with lithium hydroxide. Compound **4a** was successfully obtained over 5-steps, starting from the synthesis of hydroxymethyl diazepine (**1a**) by double nitro-Mannich reaction between *N*,*N*′-dibenzylethylenediamine, paraformaldehyde and 2-nitroethanol. Then, compound **1a** was reacted with *tert*-butyl acrylate and *t*-BuOK in THF, *via tandem* retro-Henry and Michael reactions,[16] to afford compound **2a** in good yield. Hydrogenolysis using palladium on carbon and H_2 and subsequent alkylation with methyl bromoacetate yielded the compound **3a**. Deprotection of the *tert*-butyl ester with TFA yielded the bifunctional agent derivative **4a**.

The Ln^{III}-complexes of AAZTA-C4-COO^- and AAZTA-C2-COO^- were obtained by the addition of stoichiometric amounts of $EuCl_3$ or $GdCl_3$ to the ligand solution at pH 6.5. The formation of Ln^{III}-complexes has confirmed by mass spectrometry.

Solution equilibria of the AAZTA-C2-COO^- and AAZTA-C4-COO^- ligands and its complexes

Protonation equilibria of the AAZTA-C2-COO^- and AAZTA-C4-COO^- *ligands*: The protonation constants of the ligand, defined by Eq. (1) were determined by pH-potentiometry and the values are listed in Table 1. (standard deviations are shown in parentheses). The charges of the ligands and complexes will be indicated only when they are deemed really necessary.

$$K_i^H = \frac{[H_iL]}{[H_{i-1}L][H^+]} \qquad (1)$$

where *i*=1, 2, …7. The protonation sequence of the AAZTA ligand was already fully characterized by both spectroscopic and potentiometric methods.[18] The first protonation process was shown to occur at the nitrogen atoms of the endo- and exocyclic nitrogen atoms of the ligand backbone (the protonation occurs partially at all nitrogen atoms). The second protonation takes place at the endocyclic nitrogen, whereas the first proton is moved to the exocyclic nitrogen due to the electrostatic repulsion between the protonated nitrogen atoms. Further protonations occur at the ring-carboxylate groups attached to the non-protonated endocyclic nitrogen, the non-protonated endocyclic nitrogen and/or the carboxylate pendant arms of the

exocyclic nitrogen atom, respectively (Scheme S1). According to the similarities to the parent AAZTA, the observed protonation sequence of AAZTA-C2-COO$^-$ and AAZTA-C4-COO$^-$ ligands was very similar. A comparison of the protonation constants obtained in the presence of the same background electrolyte (0.15 M NaCl, Table 1) indicated that the logK_1^H and logK_3^H values of AAZTA-C2-COO$^-$ and AAZTA-C4-COO$^-$ ligands are slightly larger than the corresponding protonation constants of the parent AAZTA. By taking into account the protonation constant of *n*-propionic acid and *n*-valeric acid (propionic acid: logK_1^H=4.53, n-valeric acid: logK_1^H=4.69, 1.0 M $NaClO_4$, 25°C),[23] one can assume that the third protonation of AAZTA-C2-COO$^-$ and AAZTA-C4-COO$^-$ occurs at the carboxylate group of the *n*-propionic and the *n*-valeric side chain. The last three protonation constants of AAZTA-C2-COO$^-$ and AAZTA-C4-COO$^-$ (logK_4^H, logK_5^H and logK_6^H) characterizing the protonation of the ring carboxylate and non-protonated exocyclic nitrogen or carboxylate groups, are very similar and comparable with the corresponding logK_i^H values (logK_3^H, logK_4^H and logK_5^H) of AAZTA ligand. The somewhat higher logK_1^H value of AAZTA-C2-COO$^-$ and AAZTA-C4-COO$^-$ might be explained by the electron donating properties of the *n*-propionic acid and the *n*-valeric side chain, which might influence the basicity of the exo- and endocyclic nitrogen atoms. It is important to note that the logK_1^H value of AAZTA and its derivative ligands determined in 0.15 M NaCl solution is significantly smaller than the value obtained in 0.1 M KCl or 0.1 M Me_4NCl solutions,[18] which might be explained by the formation of the Na^I complexes that competes with the first protonation process.

Table 1. Protonation constants of AAZTA, AAZTA-C2-COOH and AAZTA-C4-COOH ligands (25°C)

	AAZTA-C4-COO$^-$	AAZTA-C2-COO$^-$	AAZTA	
I	0.15 M NaCl		0.15 M NaCl[a]	0.1 M KCl[b]
logK_1^H	10.48 (1)	10.22 (1)	10.06	11.23
logK_2^H	6.90 (1)	6.53 (1)	6.50	6.52
logK_3^H	**4.68 (1)**	**4.33 (2)**	3.77	3.78
logK_4^H	3.73 (1)	3.62 (1)	2.33	2.24
logK_5^H	2.60 (1)	2.91 (1)	1.51	1.56
logK_6^H	1.80 (2)	2.03 (2)	–	–
logK_7^H	1.09 (3)	1.23 (3)	–	–
ΣlogK_i^H	31.27/26.59[c]	30.86/26.53[c]	24.16	25.33

[a] Ref. [19], [b] Ref. [18], [c] The protonation constant of the propionic acid and the n-valeric acid was not considered due to a negligible role in metal binding.

Complexation properties with $M^{2+/3+}$ cations: The ΣlogK_i^H values, presented in Table 1., clearly indicate that the total basicity of the AAZTA-C2-COO$^-$ and AAZTA-C4-COO$^-$ is slightly higher than of AAZTA. By taking into account the higher basicity of the AAZTA-C2-COO$^-$ and AAZTA-C4-COO$^-$, the stability constants of their Ln^{III} complexes are expected to be somewhat higher than that of the parent AAZTA complex. However, the stability constants of the Ln(AAZTA-C2-COO$^-$)$^{2-}$ and Ln(AAZTA-C4-COO$^-$)$^{2-}$ complexes might be influenced by the flexibility of the coordination cage by the presence of the side chains.

The stability and protonation constants of the metal complexes formed with the AAZTA-C2-COO$^-$ and AAZTA-C4-COO$^-$ ligand are defined by Eqs. (2) and (3).

$$K_{ML} = \frac{[ML]}{[M][L]} \quad (2)$$

$$K_{MH_iL} = \frac{[MH_iL]}{[MH_{i-1}L][H^+]} \quad (3)$$

where *i*=1, 2, …4. The protonation and stability constants of the Ca^{II}-, Zn^{II}- and Ln^{III}-complexes formed with AAZTA-C2-COO$^-$ and AAZTA-C4-COO$^-$ ligands have been calculated from the pH-potentiometric titration curves obtained at 1:1 metal/ligand concentration ratios. The best fitting was obtained by assuming the formation of ML, MHL, MH_2L, MH_3L and MH4L species in equilibrium. The formation of the deprotonated $[M(L)H_{-1}]^{n-}$ complexes takes place at pH>9.0, as indicated by the base consumption in the titration curves (M= Zn^{2+} and Cu^{2+}, n=2; M=Ln^{3+}, n=3). These processes can be interpreted by assuming a hydrolysis of the metal ion which takes place by the coordination of an OH^- ion with the formation of $[M(L)H_{-1}]^{n-}$ species. The protonation of the $[M(L)H_{-1}]^{n-}$ species is characterized by the equilibrium constant $K_{M(L)H-1}$ (Eq. (4))

$$K_{M(L)H_{-1}} = \frac{[ML]}{[M(L)H_{-1}][H^+]} \quad (4)$$

The stability and protonation constants of the Ca^{II}-, Zn^{II}, Cu^{II}- and Ln^{III}-complexes obtained by using pH potentiometric titration and UV/Vis spectrophotometric techniques are presented and compared with those of the corresponding AAZTA complexes in Table 2. The UV/Vis spectrophotometric studies of Cu^{2+} - AAZTA-C2-COO$^-$ and Cu^{2+} - AAZTA-C4-COO$^-$ systems are summarized in ESI file. The comparison of the stability constants reported in Table 2 indicates that Ca^{II}-, Zn^{II} and Ln^{III}-complexes formed by AAZTA-C2-COO$^-$ and AAZTA-C4-COO$^-$ ligands are are comparable and slightly higher than those of the corresponding AAZTA complexes due to the similar basicities of the AAZTA-C2-COO$^-$, AAZTA-C4-COO$^-$ ligands and AAZTA ligands. Interestingly, the stability constants for the Cu(AAZTA-C2-COO$^-$) and Cu(AAZTA-C4-COO$^-$) complexes are smaller by 0.6 and 1.6 log*K* unit than that of the parent Cu(AAZTA). Moreover, the stability constant of the Cu(AAZTA-C4-COO$^-$) is about 1 log*K* lower than that of the Cu(AAZTA-C2-COO$^-$). Based on the distorted octahedral structure of the Cu(AAZTA)$^{2-}$ (Cu^{II}-ion is coordinated by the exo- and endocyclic nitrogens and carboxylate oxygen atoms in equatorial positions, whereas the other endocyclic nitrogen and one of the exocyclic carboxylate oxygen atoms are in axial positions),[19] it can be reasonably assumed that the coordination of the more basic exo- and endocyclic nitrogen atoms results in the further distortion of the Cu^{II}-complexes[19] which might cause the slight decrease of the stability constant of the Cu(AAZTA-C2-COO$^-$) and Cu(AAZTA-C4-COO$^-$) upon the increase of the basicity of the exo- and endocyclic nitrogen atoms.

The stability constants of Ln(AAZTA-C2-COO$^-$) and Ln(AAZTA-C4-COO$^-$) complexes like the parent Ln(AAZTA) complexes increase from La^{3+} to Lu^{3+} (Table 2). These data clearly reflect the effect of the flexible coordination cage formed by the three nitrogen and four carboxylate oxygen atoms of the ligands that

results in an improved size match for the Ln^{3+} ions with the smaller ionic radius.

Table 2. Stability and protonation constants of AAZTA-C4-COO^-, AAZTA-C2-COO^- and AAZTA complexes formed with Ca^{2+}, Mn^{2+}, Zn^{2+} and Cu^{2+} ions (0.15 M NaCl, 25°C)

	AAZTA-C4-COO^-	AAZTA-C2-COO^-	AAZTA	
I	0.15 M NaCl		0.15 M NaCl[a]	0.1 M KCl[b]
CaL	12.05 (2)	11.91 (1)	11.75	12.76
CaHL	4.77 (2)	4.36 (1)	3.41	3.34
CaH_2L	3.27 (2)	3.58 (3)	–	–
ZnL	17.05 (3)	16.93 (3)	16.02	18.01
ZnHL	4.74 (3)	4.48 (3)	3.95	3.87
ZnH_2L	3.76 (2)	3.61 (3)	2.53	2.36
ZnH_3L	2.76 (2)	2.74 (3)	–	–
$ZnLH_{-1}$	11.39 (4)	11.44 (5)	11.36	11.25
CuL[c]	18.94 (5)	19.96 (5)	20.60	22.27
CuHL	4.79 (2)	4.54 (3)	3.86	4.00
CuH_2L	3.91 (2)	3.86 (2)	2.43	2.72
CuH_3L	2.88 (2)	2.94 (2)	1.37	–
CuH_4L	1.31 (2)	1.40 (4)	–	–
$CuLH_{-1}$	11.02 (3)	11.23 (2)	10.62	10.81
LaL	17.24 (2)	16.98 (3)	16.48	17.53
LaHL	4.68 (1)	4.36 (1)	1.90	1.97
LaH_2L	2.37 (2)	2.59 (2)	–	–
GdL	20.33 (2)	20.06 (5)	18.93	20.24
GdHL	4.74 (1)	4.45 (2)	2.18	1.89
GdH_2L	2.07 (1)	2.11 (3)	–	–
LuL	22.06 (3)	21.65 (4)	21.22	21.85
LuHL	4.65 (2)	4.47 (4)	–	–

[a] Ref. [13], [b] Ref. [19], [c] Spectrophotometry, $[H^+]$=0.01–1.0 M, I =$[H^+]$+$[Na^+]$ = 0.15 M in samples at $[H^+]$<0.15 M.

The Ca^{II}-, Zn^{II} and Ln^{III}-complexes of AAZTA-C2-COO^- and AAZTA-C4-COO^-, similarly to the behaviour shown by the analogous AAZTA complexes can be protonated at low pH values. The logK_{MHL} values of Ca^{II}-, Zn^{II}-, Cu^{II} and Ln^{III}-complexes with AAZTA-C2-COO^- and AAZTA-C4-COO^- ligands (Table 2) are very similar to the logK_3^H value of the free ligands (Table 1). The experimental evidences clearly indicate that the propionic acid and the n-valeric acid side chains of AAZTA-C2-COO^- and AAZTA-C4-COO^- ligands do not take place in the coordination to metal ions, as this functionality can protonate/deprotonate independently. At lower pH values, one and two smaller protonation constants could be determined for the Zn^{II}- and Cu^{II}-complexes, which might be explained by the presence of one or two weakly coordinated donor atom (a carboxylate oxygen) that can be protonated in the pH range of 2 to 4.

Relaxation properties of the Gd(AAZTA-C2-COO^-) and Gd(AAZTA-C4-COO^-)

Relaxivity values (r_{1p}) of Gd(AAZTA), Gd(AAZTA-C2-COO^-) and Gd(AAZTA-C4-COO^-) as a function of pH are shown in Figure 1.

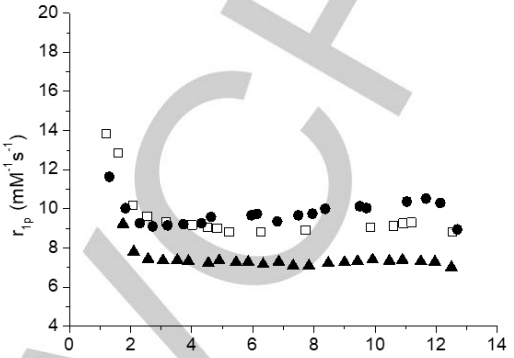

Figure 1. Relaxivity values (r_{1p}) of Gd(AAZTA) (▲), Gd(AAZTA-C2-COOH) (□) and Gd(AAZTA-C4-COOH) (●) as a function of pH ([GdL]=1.0 mM, 21 MHz, 25°C).

The relaxivity values of Gd(AAZTA-C2-COO^-) and Gd(AAZTA-C4-COO^-) are 8.8 $mM^{-1}s^{-1}$ and 9.4 $mM^{-1}s^{-1}$, respectively, at pH=7.4, 21 MHz and 298 K. The pH dependence of relaxivity shown in Figure 1 has similar behaviours for the two complexes. The r_{1p} values remain almost constant in the range of pH 2-11 while significantly increase below pH 2 and decrease above pH=11 for both complexes. The high relaxivity values obtained in strong acidic conditions have to be associated to acidic hydrolysis suffered by the complexes. At low pH, these species are highly protonated with a consequent release of the paramagnetic Gd^{3+} ions, which are characterized by high relaxivity (12.98 $mM^{-1}s^{-1}$ at 21MHz and 25°C). From pH 11-12, hydrolysis of the coordinated water molecules may take place with a consequent decrease of the relaxivity values.

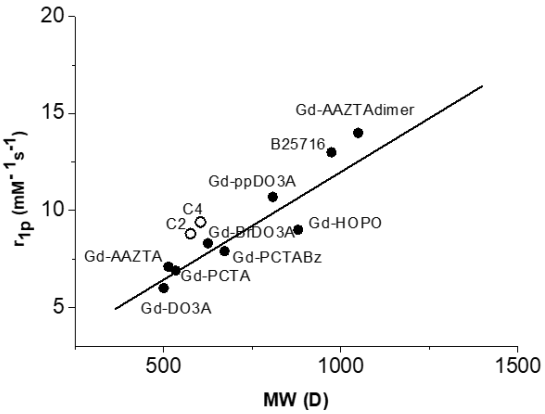

Figure 2. Molecular weight (MW) dependence of the relaxivity (0.47 T, 298 K) for typical Gd^{III}-complexes with two inner-sphere water molecules. See ref [10] and references herein.

When comparing the relaxivity values of the herein investigated Gd^{III}-complexes with those of previously reported q=2 Gd^{III}-complexes it comes evident that they are higher than what expected in the plot of relaxivity as a function of molecular weight (Figure 2). This enhancement in relaxivity can, in principle, be ascribed to either a lengthened molecular

reorientation due to some kind of aggregation and/or a contribution from second sphere water molecules.[24] The first hypothesis was checked by measuring the relaxation rate of Gd(AAZTA-C2-COO$^-$) and Gd(AAZTA-C4-COO$^-$) as a function of their concentration in the range 0.05-3.5 mM (ESI-Figure S2), at neutral pH, 25°C and 21MHz. A slight deviation from the linearity is observed, for both Gd-complexes, above concentration ca 0.1 mM, indicating the likely occurrence of a concentration dependent aggregation process. Linear fitting of data at concentration < 0.1 mM afforded relaxivity values of 7.7 and 8.6 mM^{-1}s^{-1} for Gd(AAZTA-C2-COO$^-$) and Gd(AAZTA-C4-COO$^-$), respectively. These values still fall slightly above the line of expected values on the basis of molecular weight, leading to foresee an additional contribution from second sphere water molecules.

In order to determine the kinetic parameters governing the water exchange process, the transversal relaxation rate (R_{2p}) of ^{17}O nucleus of $^{17}OH_2$ were determined by ^{17}O NMR spectroscopy at variable temperature (273 – 346 K)[25] in the presence of Gd(AAZTA-C2-COO$^-$) and Gd(AAZTA-C4-COO$^-$) complexes (Figure 3). Overall all three investigated systems show similar transverse relaxivity values (R_{2p} = $R_{2(complex)}$-$R_{2(control)}$) and are consistent with the presence of two inner sphere water molecules as for the parent Gd(AAZTA). However, while Gd(AAZTA) shows a single, pretty-defined bell-shaped profile, in the case of Gd(AAZTA-C2-COO$^-$) and Gd(AAZTA-C4-COO$^-$) derivatives, there is a clear evidence of an additional species that shows up in the low temperature measurements (273-283 K).

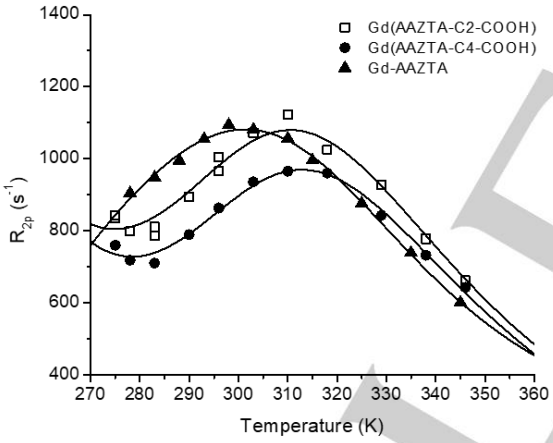

Figure 3. Comparison of the temperature dependence of the reduced transverse ^{17}O water relaxation (R_{2p}) for Gd(AAZTA-C2-COO$^-$) (□), Gd(AAZTA-C4-COO$^-$) (●) and Gd(AAZTA) (▲) at 14.09 T pH=7.4 ([GdL]=20.0 mM).

The profiles obtained for the two Gd(AAZTA) derivatives suggest that the inner sphere water molecules in these species display both fast- and slow-regime exchange rate. The analysis of the observed profiles using the modified Swift-Connick equations[26] yielded the following results: for Gd(AAZTA-C2-COO$^-$), the water molecules in fast exchange with the bulk solvent molecules are characterized by a τ_M value of 7.0 ns and weight for about 35% of the total whereas 65% of water molecules are characterized by a τ_M value of 330 ns. In the case of Gd(AAZTA-C4-COO$^-$) an analogous population distribution is observed with the corresponding values being 7.6 ns and 286 ns, respectively.

In principle, the presence of fast- and slow- exchanging populations might be ascribed either to the structurally different water molecules on the same molecule or to the presence of two distinct solution species endowed with different structures. The observation of a 35/65 distribution of the two kind of molecules between the slow and fast regime in Gd(AAZTA-C4-COO$^-$) derivative lends support to the hypothesis of the presence of the isomeric species as frequently observed in the case of solutions of macrocyclic Ln^{III} complexes.[27]

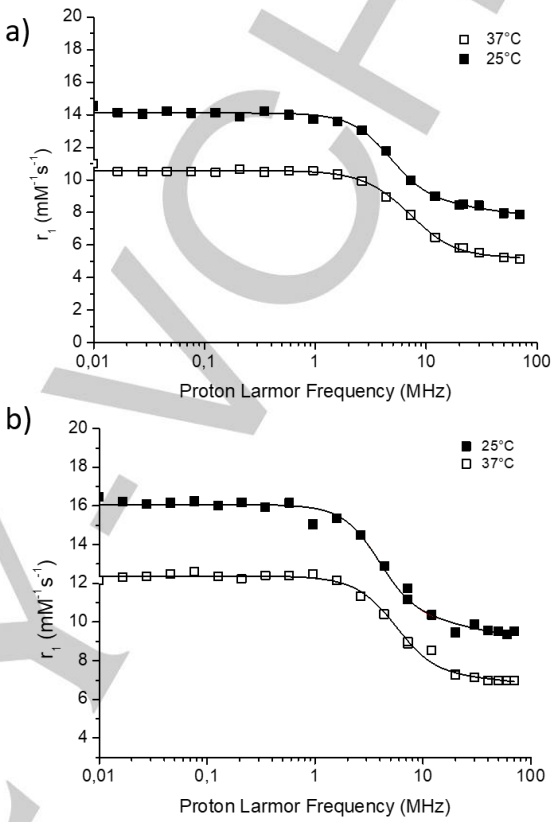

Figure 4. $1/T_1$ NMRD profile from 0.01 to 80 MHz of a 1mM aqueous solution of Gd(AAZTA-C2-COOH) (a) and Gd(AAZTA-C4-COOH) (b) at pH = 7 and 25°C (■) and 37°C (○).

To get more insight into the solution structures of the two *n*-alkyl acid derivatives of Gd(AAZTA) we went to acquire the high resolution ^{1}H-NMR spectra of the corresponding Eu^{III} and Yb^{III} complexes. Recently published VT-^{1}H NMR spectra of the Ln(AAZTA) complexes were also considered.[20] As shown in Figures S2-S6 the ^{1}H-NMR spectra showed a pattern made of half the number of methylenic protons present in each of the considered AAZTA ligands. The observed pattern did not change over an extensive range of temperature (274 – 313 K) indicating the occurrence of a fast dynamic process that hampers the detection of "frozen" structures. Actually, by passing from water to a D_2O/DMSO-d_6 (60/30 vol %) mixture it was possible to acquire spectra down to 248 K (Figures S2 and S5). Inspection in the lowest temperature spectra allowed to access differences in the broadening of the resonances that may be suggestive of an incipient coalescence process. The observed behaviour is taken as an additional support for the hypothesis for the presence, in solution, of two interconverting isomers, differing for the exchange regime of the coordinated water molecules.

More information on the determinants of the observed relaxivity was obtained recording the $1/T_1$ NMRD profiles over an extended range of magnetic field strengths (0.01-80 MHz as

proton Larmor Frequency). The NMRD profiles measured at neutral pH, 25°C and 37°C for Gd(AAZTA-C2-COO$^-$) and Gd(AAZTA-C4-COO$^-$), are shown in Figure 4. Experimental data were fitted using the SBM theory to extract the relevant relaxometric parameters (Δ^2, τ_V and τ_R) reported in Table 3. In the fitting procedure, the values of τ_M for the two derivatives were kept fixed to the weighted average of the values determined by ^{17}O-NMR-R_{2p}.

Table 3. Relaxation parameters of the Gd(AAZTA-C2-COO$^-$), Gd(AAZTA-C4-COO$^-$) and Gd(AAZTA) complexes as derived from fitting of $^{17}OR_{2p}$ vs temp. and NMRD profiles (25°C).

		Gd(AAZTA-C4-COOH)	Gd(AAZTA-C2-COOH)	Gd(AAZTA)[g]
r_{1p} (0.47T, 298K)		9.4	8.8	7.1
$\Delta^2 \times 10^{19}$ / s^{-2} [a]		2.3±0.21	3.2±0.24	2.15
τ_V / ps [b]		32.6±2.9	26.1±1.7	31.0
τ_R / ps [c]		115±2.2	92±1.5	74
τ_M / ns [d]	species 1	7.6 (35%)	7.0 (35%)	90
	species 2	286 (65%)	331 (65%)	
q[e]		2	2	2
q_{SS}[f]		1	1	0

[a] Squared mean transient zero-field splitting (ZFS) energy as obtained from fitting of NMRD profiles. [b] Correlation time for the collision-related modulation of the ZFS Hamiltonian as obtained from fitting of NMRD profiles. [c] Re-orientational correlation time as obtained from fitting of NMRD profiles. [d] Exchange life-time of the coordinated water molecules as obtained from fitting of $^{17}OR_{2p}$vsT profiles of Fig.3 . [e] Number of inner sphere water molecules as obtained from fitting of NMRD profiles. [f] Number of second sphere water molecules as obtained from fitting of NMRD profiles., [g] Ref.[17]

The best fitting of experimental data afforded the presence of one second sphere water molecule for both Gd(AAZTA-C2-COO$^-$) and Gd(AAZTA-C4-COO$^-$) which was not present in the parent Gd(AAZTA). This result supported the suggestion related to the observation that the proton relaxivity values at 21.5 MHz (Figure 2) fall slightly above the line of expected values calculated on the basis of the molecular weights. This additional contribution from second sphere water molecules is likely related to the presence on the herein reported complexes of the acidic alkyl function, which is expected to enhance the overall hydrophilic character of the complexes.

Transmetallation of Gd(AAZTA-C2-COO$^-$) and Gd(AAZTA-C4-COO$^-$) complexes with Cu^{2+}

Besides the high thermodynamic stability, GBCAs must be characterized by high kinetic inertness in order to avoid the *in vivo* dissociation of the Gd^{III}-complexes. Actually it has been realized that the kinetic inertness is more important than the absolute value of the stability constant for the *in vivo* applications of Gd^{III} complexes.[3,28–30] Body fluids are very complex systems and the *in vivo* study of the rate of dissociation reactions of Gd^{III} complexes is considered a difficult task.[31–33] However, *in vitro* studies are usually quite suitable to predict the kinetic behaviour of the Gd^{III} complexes under *in vivo* conditions. The kinetic inertness of the Gd(AAZTA) was assessed by investigating the rates of the transmetallation reaction with the use of Cu^{2+} or Eu^{3+} as exchanging ions.[18] For a direct comparison of the kinetic properties of Gd(AAZTA-C2-COO$^-$), Gd(AAZTA-C4-COO$^-$) and Gd(AAZTA), the same method and identical conditions were used as previously used for Gd(AAZTA).[18] The rates of the transmetallation reactions were studied by spectrophotometry in the presence of Cu^{2+} as exchanging metal ion. Mechanism proposed for the transmetallation reactions of the Gd(AAZTA-C2-COO$^-$) and Gd(AAZTA-C4-COO$^-$) with Cu^{2+} are summarized in Scheme 4. Experimental details and equations used to evaluate the kinetic parameters are summarized in ESI. The rate and equilibrium constants that characterize the transmetalation reaction of Gd(AAZTA-C2-COO$^-$) and Gd(AAZTA-C4-COO$^-$) are shown and compared with those of Gd(AAZTA) in Table 4. In our experimental condition (pH=2.8 – 5.0) the dominating species is Gd(HL) with the protonated *n*-propionate and *n*-valerate pendants.

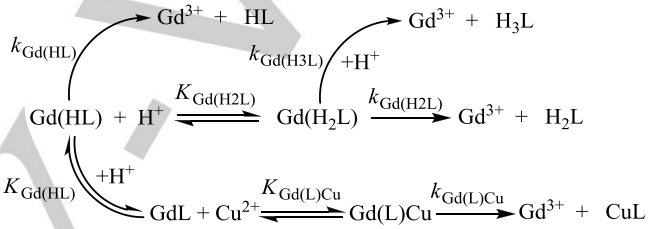

Scheme 4. Proposed mechanism of the transmetallation reactions for the Gd(AAZTA-C2-COO$^-$) and Gd(AAZTA-C4-COO$^-$) complexes. The lower and the last upper paths are valid for the Gd(AAZTA-C2-COO$^-$) and Gd(AAZTA-C4-COO$^-$) complex, respectively.

Table 4. Rate (k_i) and equilibrium constants (K_i) and half-lives ($t_{1/2}$=ln2/k_d) for the transmetallation reactions of Gd(AAZTA-C4-COO$^-$), Gd(AAZTA-C2-COO$^-$) and Gd(AAZTA) complexes (25°C)

	Gd(AAZTA-C4-COO$^-$)	Gd(AAZTA-C2-COO$^-$)	Gd(AAZTA)[a]
I	0.15 M NaCl		0.1 M KCl[b]
k_{GdHL} / s^{-1}	(7 ± 2)×10^{-6}	(2 ± 2)×10^{-5}	4.5×10^{-3}
$k_{Gd(H2L)}$ / s^{-1}	(2.3 ± 0.2)×10^{-3}	(2.2 ± 0.1)×10^{-3}	–
$k_{Gd(H3L)}$ / s^{-1}	1.2 ± 0.3	–	–
$k_{Gd(L)Cu}$ / s^{-1}	–	(1.0 ± 0.1)×10^{-5}	2.1×10^{-5}
$K_{Gd(HL)}$ / M^{-1}	54954 (pH-pot.)	28183 (pH-pot.)	233
$K_{Gd(H2L)}$ / M^{-1}	118 (pH-pot.)	128 (pH-pot.)	–
$K_{Gd(L)Cu}$ / M^{-1}	–	166 ± 40	9
k_d / s^{-1} pH=7.4	1.4×10^{-8}	2.3×10^{-8}	4.0×10^{-8}
$t_{1/2}$ / h pH=7.4	1.3×10^4	1.0×10^4	4.3×10^3

[a] Ref. [18]

According to the proposed mechanism, the dissociation of the Gd(AAZTA) derivatives might take place by the proton- and metal-assisted pathways.[18] The proton assisted dissociation of the Gd^{III}-complexes generally takes place by the protonation of the complexes via the formation of protonated intermediates. The protonation of the Gd(AAZTA) derivatives presumably

occurs on the carboxylate groups. The dissociation that might take place via proton transfer from the carboxylate group to the nitrogen atom, results in the displacement of the Gd^{3+} ion from the coordination cage and the release of the Gd^{3+}. The $k_{Gd(HL)}$ rate constants characterizing the dissociation rate of the monoprotonated Gd(AAZTA-C2-COOH) and Gd(AAZTA-C4-COOH) species are about 44 and 1500 times smaller that that of monoprotonated Gd(HAAZTA). Since the protonation of the Gd(AAZTA-C2-COO^-) and Gd(AAZTA-C4-COO^-) takes place on the distant *n*-propionate and the *n*-valerate side chain, the proton transfer to the nitrogen atom is less probable than that of Gd(HAAZTA) species with the protonated carboxylate group of the AAZTA skeleton. On the other hand, the dissociation rate of the double protonated Gd(HAAZTA-C2-COOH) and Gd(HAAZTA-C4-COOH) species ($k_{Gd(H2L)}$) are comparable with the $k_{Gd(HL)}$ value of the Gd(HAAZTA) species. Since the second protonation of Gd(AAZTA-C2-COO^-) and Gd(AAZTA-C4-COO^-) and the first protonation of Gd(AAZTA) occur on the carboxylate group of the AAZTA unit, the dissociation of these protonated Gd^{III}-complexes might takes place by the similar probability. However, the somewhat lower $k_{Gd(H2L)}$ values of Gd(HAAZTA-C2-COOH) and Gd(HAAZTA-C4-COOH) than that of $k_{Gd(HL)}$ of Gd(HAAZTA) may be explained by the interaction between the Gd^{3+} ion and the basic nitrogen atoms of AAZTA-C2-COO^- and AAZTA-C4-COO^-. The stability constants of the heter-dinuclear Gd(AAZTA-C2-COO^-)Cu intermediate ($K_{Gd(L)Cu}$) is about 16 times higher than that of Gd(AAZTA)Cu, which can be explained by the coordination of the Cu^{II}-ion by the more basic *n*-propionate side in Gd(AAZTA-C2-COO^-)Cu intermediate. $k_{Gd(L)Cu}$ rate constant, characterizing the dissociation of dinuclear Gd(AAZTA-C2-COO^-)Cu intermediate is about two times smaller than that of Gd(AAZTA)Cu. Because of the stronger interaction, the functional groups of the AAZTA-C2-COO^- ligand are transferred with the much smaller rate from the Gd^{III} to the attacking Cu^{II} ion in respect to what was found in the case of Gd(AAZTA). This hypothesis is further supported by the lack of the Cu^{2+} assisted dissociation of the Gd(AAZTA-C4-COO^-) complex due to the sronger coordination of the Gd^{3+} ion with the more basic nitrogen atoms of the ligand. Somewhat larger kinetic inertness of Gd(AAZTA-C4-COO^-) and Gd(AAZTA-C2-COO^-) complexes is also confirmed by the calculated dissociation rate (k_d) and half-life ($t_{1/2}$) values at pH=7.4. k_d and $t_{1/2}$ values in Table 4 reveal that the dissociation of Gd(AAZTA-C2-COO^-) and Gd(AAZTA-C4-COO^-) complexes slightly slower than that of Gd(AAZTA).

Conclusions

Two functionalized Gd(AAZTA) derivatives have been successfully synthetized and characterized. They appear promising systems for further conjugation to substrates of interest. Moreover it was found that they show improved relaxation properties and slightly better thermodynamic and kinetic behaviour when compared with those ones of the parent Gd(AAZTA). Therefore, the body of these results leads to conclude that these complexes are good candidates as contrast agents for further MRI applications either by their own or as systems for the design of targeting agents. Relaxometric studies demonstrated that these complexes presented improved relaxivity values (r_{1p} = 8.8 $mM^{-1}.s^{-1}$ and 9.4 $mM^{-1}.s^{-1}$ for the derivatives C_2 and C_4 spaced, respectively, in comparison to Gd(AAZTA) (r_{1p} = 7.1 $mM^{-1}.s^{-1}$). ^{17}O- and ^1H-NMR spectra results suggest the presence in solution of species containing water molecules in two distinct motion regimes. The observation of fast and slow water exchanging isomers is not uncommon in lanthanide(III) macrocyclic complexes and it is usually accompanied by the observation of the corresponding sets of signals in the corresponding ^1H-NMR spectra of the analogs with other Ln^{III}-ions. Herein the interconversion appears too fast to be slowed down in the high resolution NMR spectra.

A corollary to these observations is that, for the first time to our knowledge, it has been possible, in the field of Ln^{III} containing complexes, to extract fundamental information on the presence of two interconverting isomers from the ^{17}O NMR data when the high resolution NMR spectra were completely non informative.

Experimental

1. General

All standard chemicals were acquired from Merck and VWR. The new compounds were characterized by using ^1H and ^{13}C NMR. ^1H and ^{13}C-NMR spectra were recorded at 298K on a Bruker spectrometer (600 MHz for ^1H). UPLC (Ultra-performance liquid chromatography)-analytical characterizations were carried out using a Waters UPLC-*H*-Class system equipped with Acquity QDa MS detector and dual-wavelength UV/Vis TUV detector. Purification by using HPLC was performed with a system equipped with Waters 2767 autosampler and autoinjector, Waters 2525 pumps, Waters 3100 MS Detector and Waters 2998 photodiode array (PDA) detector, on Atlantis dC18 OBD Prep Column, 100Å, 5 µm, 19 mm X 100 mm. Water 0.1% TFA (A) and acetonitrile 0.1% TFA (B) were used as eluents.

2. Synthesis of H_4AAZTA-C4-COOH ligand (Scheme 2)

Compound 1: N,N'-dibenzylethylenediamine (28.6 mmol, 6.7 mL) was suspended in EtOH (50 mL) and the mixture was stirred until a clear solution was obtained. Paraformaldehyde (86 mmol, 2.6 g) was added and the suspension was stirred and heated at 80°C for 1.5 h. The solution of 6-nitrohexanoic acid methyl ester (28.6 mmol, 5 g) in EtOH (10 mL) was added dropwise. The new solution was left to cool to room temperature and stirred for 18 hours. The mixture was evaporated and the residue dissolved in ethyl acetate (EtOAc) was purified by flash chromatography (silica gel column, 90:10 petroleum ether/EtOAc) to give 1 as a pale yellow oil (7.4 g, 60%). ^1H NMR ($CDCl_3$) : δ 7.32 (m, 10H), 3.76 (d, 2H, *J*= 13Hz), 3.67 (s, 3H), 3.60 (d, 2H, *J*=13Hz), 3.53 (d, 2H, J=14.2), 2.98 (d, 2H, *J*=14.2), 2.64 (m, 4H), 2.13 (t, 2H, *J*=7.5), 1.59 (m, 2H), 1.32 (m, 2H), 0.79 (m, 2H). ^{13}C NMR (CDCl3): δ 173.1, 138.5, 128.5, 127.6, 126.5, 94.1, 63.4, 60.8, 58.1, 50.9, 36.0, 32.9, 23.9, 21.9. ESI-MS (m/z): $[M+H]^+$ 440.5 (obsd.), 440.5 (calcd. for $C_{25}H_{34}N_3O_4$).

Compound 3: Palladium on carbon (1.0 g) was slowly added to a solution of compound **1** (15.5 mmol; 6.8 g) in MeOH (300 mL). The suspension was stirred at 40°C for 5 h under hydrogen atmosphere. The suspension was filtered on a bed of Celite and concentrated *in vacuo.* The residue was dissolved in acetonitrile (MeCN) (75 mL) and then freshly ground K_2CO_3 (80.2 mmol; 11.0 g) and Na_2SO_4 (15.0 mmol; 2.1 g) were added. *t*-Butyl bromoacetate (71.0 mmol; 10.4 g) was added and the orange mixture was stirred and heated at 80°C for 20 hours. The mixture was filtered, evaporated and the residue was purified by chromatography (silica gel column, 30: 5 *n*-hexane/EtOAc to give a pale yellow oil (6.0 g; 57%).^1H NMR ($CDCl_3$): δ 3.66 (s, 3H; OCH_3), 3.61 (s, 4H), 2.69-3.01 (br, 6H), 2.32 (t, 2H, *J*= 7.5 Hz), 1.53-1.64 (br, 6H), 1.45 (s, 36 H). ^{13}C NMR ($CDCl_3$): δ 173.3. 172.0, 81.3, 80.4, 65.5, 62.8, 61.5, 60.6, 51.2, 50.8, 35.8, 33.2, 27.5, 24.8, 21.5. ESI-MS (m/z): $[M+H]^+$ 686.6 (obsd.), 686.5 (calcd. for $C_{35}H_{64}N_3O_{10}$);

Compound 4: A 1 M solution of LiOH (23.0 mmol; 23.0 mL) was added dropwise to a solution of compound **3** (2.9 mmol; 2.0 g) in tetrahydrofuran (THF) (50 mL) cooled at 0°C. The solution was then stirred at room temperature for 28 h. The pH was brought to 7.0 by addition of HCl 6 M. Water (45 mL) was added and THF was evaporated. The aqueous residue was extracted with EtOAc (3 x 75 mL). The organic phases were collected, dried with Na_2SO_4, filtered and concentrated *in vacuo*. The crude was purified by chromatography (silica gel column, 3:2 *n*-hexane/ EtOAc) to give 4 as a pale yellow oil. (1.0 g; 54%). ^{1}H NMR ($CDCl_3$): δ 3.63 (s, 4H), 3.16 (br, 6H), 2.41 (t, 2H), 1.61-1.67 (br, 6H), 1.48 (s, 36 H). ^{13}C NMR ($CDCl_3$): δ 178.7, 173.2, 171.0, 81.6, 80.7, 65.3, 63.3, 61.5, 60.3, 37.4, 34.3, 29.0, 27.5, 21.4. ESI-MS (m/z): $[M+H]^+$ 672.6 (obsd.), 672.4 (calcd. for $C_{34}H_{62}N_3O_{10}$); $[M+Na]^+$ 694.6 (obsd.), 694.8 (calcd).

Compound 5 (H4AAZTA-C4-COOH): Trifluoroacetic acid (20 mL) was added dropwise to a solution of **4** (1,0 g, 1.50 mmol) and triisopropylsilane (0.6 mL) in CH_2Cl_2 (5 mL) cooled to 0-5 °C. The solution was stirred at room temperature for 20 h, then evaporated. The residue dissolved in H_2O (5 mL) was purified by HPLC under isocratic conditions (98:2, A:B) at a flow rate of 20 mL/min. The pure product was obtained as a white powder (0.40 g, yield 60%) and characterized by UPLC-UV-MS-ESI(+) using a Acquity UPLC HSS T3 Column, 100Å, 1.8 µm, 2.1 mm X 100 mm and 0.05% TFA in water (A) and 0.05% TFA in acetonitrile (B) as solvents. Elution: initial condition 0% B, isocratic 0 % B over 0.56 min, gradient 0-10% B over 2.5 min, 10-30% B over 6 min, 30-100% B over 10 min, flow rate 0.4 mL/min and UV detection at 220 nm (t_R, retention time = 3.9 min, purity 95.0%). ^{1}H NMR (D_2O): δ 3.80 (d, 4H, *J*= 5.1 Hz), 3.71 (s, 4H), 3.60 (m, 2H), 3.44 (s, 6H), 2.31 (t, 2H, J=7.2), 1.50 (m, 2H), 1.26 (m, 2H). ^{13}C NMR (D_2O): δ 177.8, 175.6, 169.8, 61.9, 59.3, 57.8, 51.8, 51.5, 33.2, 32.6, 23.8, 21.4. ESI-MS (m/z): $[M+H]^+$ 448.3 (obsd.), 448.4 (calcd. for $C_{18}H_{30}N_3O_{10}$).

3. Synthesis of H_4AAZTA-C2-COOH (Scheme 3)

Compound 1a: N,N'-dibenzylethylenediamine (22.0 mmol, 5.3 mL) was suspended in EtOH (50 mL) and the mixture was stirred until a clear solution was obtained. Paraformaldehyde (66.0 mmol, 2.0 g) was added and the suspension was stirred and heated at 80°C for 1.5 h. The solution of 2-nitroethanol (22.0 mmol, 2 g) in EtOH (10 mL) was added dropwise. The new solution was left to cool to room temperature and stirred for 18 hours. The mixture was evaporated and the residue dissolved in ethyl acetate (EtOAc) was purified by flash chromatography (silica gel column, 80:20 petroleum ether/EtOAc) to give 1 as a pale yellow oil (7.0 g, 90%). ^{1}H NMR ($CDCl_3$) : δ 7.33 (m, 10H), 3.74 (d, 2H, *J*= 13Hz), 3.70 (s, 2H), 3.65 (d, 2H, *J*=13Hz), 3.53 (d, 2H, J=14.4), 3.05 (d, 2H, *J*=14.3), 2.70 (m, 2H), 2.63 (m, 2H). ^{13}C NMR (CDCl3): δ 138.0, 128.3, 127.7, 126.7, 94.0, 65.0, 63.1, 58.37, 58.0. ESI-MS (m/z): $[M+H]^+$ 356.2 (obsd.), 356.2 (calcd. for $C_{20}H_{26}N_3O_3$).

Compound 2a: Compound **1a** (18.0mmol, 6.3g) was dissolved in dry THF (40 mL), *tert*-butyl acrylate (5.3 mL, 36.0 mmol) was added and the mixture was stirred at room temperature for 5 minutes. *t*-BuOK (2.4 g, 21.6 mmol) was added to the solution, and stirring was continued at room temperature for 3 hours. After removal of the solvent under reduced pressure, the residue was taken up in methanol and purified by chromatography (silica gel column, 90:10 petroleum ether/EtOAc) to give 2a as a pale yellow oil (3.9 g, 48%). ^{1}H NMR ($CDCl_3$): δ 7.31 (m, 10H), 3.76 (d, 2H, *J*= 12.5Hz), 3.61 (d, 2H, *J*= 12.7Hz), 3.50 (d, 2H, *J*=14Hz), 2.98 (d, 2H, J=14), 2.61 (m, 4H), 1.96 (m, 2H), 1.74 (m, 2H), 1.43 (s, 9H). ^{13}C NMR (CDCl3): δ 170.3, 138.3, 128.3, 127.6, 126.6, 93.4, 80.0, 63.2, 61.0, 57.9, 31.0, 28.4, 27.3. ESI-MS (m/z): $[M+H]^+$454.3 (obsd.), 454.3 (calcd. for $C_{26}H_{36}N_3O_4$).

Compound 3a: Palladium on carbon (0.3 g) was slowly added to a solution of compound **2a** (1.3 g, 2.8 mmol) in MeOH (50 mL). The suspension was stirred at 40°C for 5 h under hydrogen atmosphere. The suspension was filtered on a bed of Celite and concentrated *in vacuo*.The residue was dissolved in acetonitrile (MeCN) (50 mL) and then freshly ground K_2CO_3 (2.0 g, 15 mmol) and Na_2SO_4 (0.36 g, 2.6 mmol) were added. Methyl bromoacetate (1.24 mL, 13.2 mmol) was added and the mixture was stirred and heated at 80°C for 20 hours. The mixture was filtered, more K_2CO_3 (2.0 g, 15 mmol), Na_2SO_4 (0.36 g; 2.6 mmol) and methyl bromoacetate (0.62 mL, 6.6 mmol,) were added and the new mixture heated at 80°C for 12 h. The mixture was filtered, evaporated and the residue was purified by chromatography (silica gel column, 30: 5 *n*-hexane/EtOAc to give a pale yellow oil (0.7 g; 47%).^{1}H NMR ($CDCl_3$): δ 3.75 (s, 4H), 3.69 (s, 6H), 3.67 (s, 6H), 3.36 (s, 4H), 3.01 (d, 2H, *J*= 14.3Hz) 2.8 (m, 2H), 2.69 (m, 4H), 2.35 (m, 2H), 1.84 (m, 2H), 1.43 (s, 9H). ^{13}C NMR ($CDCl_3$): δ 172.9, 172.6, 171.0, 79.3, 63.6, 62.1, 60.4, 58.3, 50.8, 50.6, 31.3, 28.0, 27.4. ESI-MS (m/z): $[M+H]^+$ 532.2 (obsd.), 532.3 (calcd. for $C_{24}H_{42}N_3O_{10}$).

Compound 4a: Trifluoroacetic acid (2 mL) was added dropwise to a solution of **3a** (0,5 g, 0.94 mmol) and triisopropylsilane (0.050 mL) in CH_2Cl_2 (2mL) cooled to 0-5 °C. The solution was stirred at room temperature for 1 h. The mixute was co-evaporated with CH_2Cl_2 (3 ×10mL) and taken into next step without further purification. ^{1}H NMR ($CDCl_3$): δ 3.89 (s, 2H), 3.83 (s, 2H), 3.79 (s, 6H), 3.75 (s, 6H), 3.71 (s, 4H), 3.47-3.31 (m, 6H), 3.16 (d, 2H, *J*=14.5Hz), 2.42 (t, 2H, *J*= 7.4), 1.79 (t, 2H, *J*= 7.4). ^{13}C NMR ($CDCl_3$): δ 175.4, 173.8, 167.3, 61.4, 60.0, 57.4, 52.9, 51.9, 51.8, 49.9, 29.2, 27.2. ESI-MS (m/z): $[M+H]^+$ 476.4 (obsd.), 476.2 (calcd. for $C_{20}H_{34}N_3O_{10}$).

Compound 5a (H4AAZTA-C2-COOH): A 1 M solution of LiOH (20.0 mmol; 20.0 mL) was added dropwise to a solution of compound **3a** (0.6 mmol; 0.4 g) in tetrahydrofuran (THF) (40 mL) cooled at 0°C. The solution was then stirred at room temperature for 28 h. The pH was brought to 7.0 by addition of HCl 6 M. Water (45 mL) was added and THF was evaporated. The aqueous residue was purified by HPLC under isocratic conditions (98:2, A:B) at a flow rate of 20 mL/min. The pure product was obtained as a white powder (0.10 g, yield 39%) and characterized by UPLC-UV-MS-ESI(+) using method described for compound 5, (t_R = 2.5 min, purity 92.0%). ^{1}H NMR (D_2O): δ 3.80 (s, 4H), 3.71 (s, 4H), 3.40 (m, 2H), 3.32 (s, 6H), 2.38 (t, 2H, *J*=8.0), 1.68 (t, 2H, *J*= 8.0). ^{13}C NMR (D_2O): δ 176.3, 176.1, 170.4, 61.3, 59.2, 57.7, 52.2, 50.2, 28.5, 27.1. ESI-MS (m/z): $[M+H]^+$ 420.2 (obsd.), 420.1 (calcd. for $C_{16}H_{26}N_3O_{10}$).

4. Synthesis of Ln^{III}-complexes

Aqueous solutions of $GdCl_3$ or $EuCl_3$ and ligands were mixed at 1:1 concentration ratio ([$GdCl_3$]=[$EuCl_3$]=[H_4AAZTA-C4-COOH]=[H_4AAZTA-C2-COOH]=50 mM). The solutions were stirred for 4 hours. The pH of the solutions was maintained 7 by the addition of solid NaOH. The occurrence of residual free Ln^{3+} ion was assessed by UV-Vis spectroscopy using the *xylenol orange* test [34]. The amount of the residual free Ln^{3+} ion was less than 0.3% (mol/mol). The Ln^{III}-complexes were characterized by direct-infusion method using ESI-MS (*Waters 3100*) in negative ion mode Gd(AAZTA-C2-COOH): ESI- MS (-): m/z: calculated for $C_{16}H_{21}GdN_3O_{10}$ $[M-H]^-$: 573.0, found: 573.1; Eu(AAZTA-C2-COOH): ESI- MS (-): m/z: calculated for $C_{16}H_{21}EuN_3O_{10}$ $[M-H]^-$: 568.0, found: 568.1; Gd(AAZTA-C4-COOH): ESI- MS (-): m/z: calculated for $C_{18}H_{25}GdN_3O_{10}$ $[M-H]^-$: 601.0, found: 601.2; Eu(AAZTA-C4-COOH): ESI-MS (-): m/z: calculated for $C_{18}H_{25}EuN_3O_{10}$ $[M-H]^-$: 596.0, found: 596.2. The concentration of the Gd^{III}-complexes was determined by ^{1}H-NMR relaxometry after remineralization for 24 hours at 120°C in concentrated HCl solution (37%, v/v).

5. Thermodynamic studies

Materials: The chemicals used for the experiments were of the highest analytical grade. The concentration of the $CaCl_2$, $ZnCl_2$, $CuCl_2$ and $GdCl_3$ solutions were determined by complexometric titration with standardized Na_2H_2EDTA and *xylenol orange* ($ZnCl_2$, and $LnCl_3$), *murexid* ($CuCl_2$) and *Patton & Reeder* ($CaCl_2$) as indicators. The concentration of the H_4AAZTA, H_4AAZTA-C2-COOH and H_4AAZTA-C4-COOH was determined by pH-potentiometric titration in the presence and absence of a large (40-fold) excess of $CaCl_2$. The pH-potentiometric titrations were made with standardized 0.2 M NaOH.

Equilibrium measurements: The stability and protonation constants of Ca^{II}, Zn^{II} and Ln^{III} -complexes formed with AAZTA-C2-COO^- and AAZTA-C4-COO^- ligands were determined by pH-potentiometric titration. The metal-to-ligand concentration ratio was 1:1 (the concentration of the ligand was generally 0.002 M). In calculating the equilibrium constants of the metal complexes, the best fitting of the NaOH - pH data pairs, were obtained by assuming the formation of ML, MHL, MH_2L, MH_3L, MH_4L and MLH_{-1} complexes in the 1.7-12.0 pH range. For the pH measurements and titrations, *Metrohm 888 Titrando* titration workstation *Metrohm-6.0234.110* combined electrode was used. Equilibrium measurements were carried out at a constant ionic strength (0.15 M NaCl) in 6 ml samples at 25 °C. The solutions were stirred, and N_2 was bubbled through them. The titrations were made in the pH range of 1.7-12.0. KH-phthalate (pH=4.005) and borax (pH=9.177) buffers were used to calibrate the pH meter, For the calculation of $[H^+]$ from the measured pH values, the method proposed by *Irving et al.* was used as follows.[35] A 0.01M HCl solution was titrated with standardized NaOH solution at 0.15 M NaCl ionic strength. The differences (*A*) between the measured (pH_{read}) and calculated pH (-log$[H^+]$) values were used to obtain the equilibrium H^+ concentration from the pH values measured in the titration experiments (*A*=0.024). For the equilibrium calculations, the stoichiometric water ionic product (pK_w) was also needed to calculate $[OH^-]$ values under basic conditions. The V_{NaOH} – pH_{read} data pairs of the HCl – NaOH titration obtained in the pH range 10.5 – 12.0 were used to calculate the pK_w value (pK_w=13.85).

The stability constant of the Cu(AAZTA)$^{2-}$, Cu(AAZTA-C2-COO^-)$^{3-}$ Cu(AAZTA-C4-COO^-)$^{3-}$ complexes was determined by spectrophotometry studying the competition reaction between the Cu^{2+} and H^+ for the AAZTA, AAZTA-C2-COO^- and AAZTA-C4-COO^- at the absorption band of Cu(AAZTA)$^{2-}$, Cu(AAZTA-C2-COO^-)$^{3-}$ Cu(AAZTA-C4-COO^-)$^{3-}$ in the wavelength range of 400-800 nm. The concentration of Cu^{2+}, AAZTA, AAZTA-C2-COO^- and AAZTA-C4-COO^- was 0.002 M, while that of the H^+ was varied between 0.01 and 1.0 M (6 samples). The H^+ concentration in the samples was adjusted with the addition of calculated amounts of 3 M HCl. The ionic strength of samples was adjusted to 0.15 M (H^+]≤0.15 M→[Na^+]+[H^+]=0.15 M). The samples were kept at 25 °C for 7 days in order to attain the equilibrium (the time needed to reach the equilibria was determined by spectrophotometry). The absorbance values of the samples were determined at 11 wavelengths (575, 595, 615, 635, 655, 675, 695, 715, 735, 755 and 775 nm). For the equilibrium calculations, the protonation constants of the Cu(AAZTA)$^{2-}$, Cu(AAZTA-C2-COO^-)$^{3-}$ Cu(AAZTA-C4-COO^-)$^{3-}$ and the molar absorptivities of the Cu^{2+}, CuL, Cu(HL), Cu(H_2L), Cu(H_3L) and Cu(H_4L) species were used. The protonation constants of the complexes Cu(AAZTA)$^{2-}$, Cu(AAZTA-C2-COO)$^{3-}$ Cu(AAZTA-C4-COO)$^{3-}$ were determined by pH-potentiometric titrations, made at 1:1 metal to ligand concentration ratios. The molar absorptivities of the Cu^{2+}, CuL, Cu(HL), Cu(H_2L), Cu(H_3L) and Cu(H_4L) species were determined at 11 wavelengths (575, 595, 615, 635, 655, 675, 695, 715, 735, 755 and 775 nm) by recording the spectra of 1, 2 and 3 mM Cu(AAZTA)$^{2-}$, Cu(AAZTA-C2-COO^-)$^{3-}$ Cu(AAZTA-C4-COO^-)$^{3-}$ solutions in the pH range 1.7 – 6.0 (0.15 M NaCl, 25°C). The pH was adjusted by stepwise addition of concentrated NaOH or HCl. The spectrophotometric measurements were made with the use of *PerkinElmer Lambda 365* UV-Vis spectrophotometer at 25 °C, using 1.0 cm cells. The protonation and stability constants were calculated with the PSEQUAD program.[36]

6. Kinetic studies of thee trans-metallation reactions

The kinetic inertness of the Gd(AAZTA-C2-COO^-)$^{2-}$ and Gd(AAZTA-C4-COO^-)$^{2-}$ complexes was characterized by the rates of the exchange reactions taking place between the GdL and Cu^{2+}. The transmetallation reactions with Cu^{2+} were studied by spectrophotometry, following the formation of the Cu^{II} complexes at 300 nm with a *PerkinElmer Lambda 365* UV-Vis spectrophotometer. The concentration of the GdL complexes was 1×10^{-3} M, while the concentration of the Cu^{2+} was 20, 30, 40 and 50 times larger, in order to guarantee pseudo-first-order conditions. The temperature was maintained at 25°C and the ionic strength of the solutions was kept constant, 0.15 M for NaCl. The exchange rates were studied in the pH range about 2.8 – 5.0. For keeping the pH values constant, monochloroacetic acid (pH range 2.8 – 3.1), *N,N'*-dimethylpiperazine (pH range 3.1 – 4.1) and *N*-methylpiperazine (pH range 4.1 – 5.2) buffers (0.01 M) were used. The pseudo-first-order rate constants (k_d) were calculated by fitting the absorbance data to Eq. (5)

$$A_t = (A_0 - A_p)e^{-k_d t} + A_p \qquad (5)$$

where A_t, A_0 and A_p are the absorbance values at time *t*, the start of the reaction and at equilibrium, respectively.

7. Relaxometric studies

The observed longitudinal water protons relaxation rates (R_{1obs}) were measured using a Stelar Spinmaster (Mede, Pavia, Italy) spectrometer operating at 0.47 T and employing a standard inversion-recovery (IR) pulse sequence (16 experiments, 2 scans). A typical 90° degree pulse width was 3.5 µs and the reproducibility for the longitudinal relaxation times (T_1) were ±0.5%. NMRD profiles were obtained using a Stelar SpinMaster FFC-NMR relaxometer from 0.01-20 MHz and a Bruker WP80 NMR electromagnet for variable higher-field measurements (21.5 - 80 MHz), both equipped with a Stelar VTC-91 air-flow heater equipped with copper/constant thermocouple (uncertainty ±0.1°C) for temperature control. .

8. NMR studies

The VT-^{1}H NMR spectra of Eu^{III}- and Yb^{III}-complexes were recorded on the Bruker Avance III (9.4 T) and Avance 600 (14.09 T) spectrometer, equipped with 5 mm probe and using a D_2O solution as internal lock. The temperature was controlled with Bruker thermostating units, and high resolution spectra have been acquired by varying the temperature from 278 K to 350 K. Variable temperature ^{17}O NMR measurements were performed with Bruker Avance spectrometer, equipped with a 5mm probe and using a capillary containing D_2O as external lock. The experimental settings were: spectral width 1000 Hz, 90° degree pulse (7 µs), acquisition time 10 ms, 1000 scans, and no sampling spinning. Aqueous solutions containing 2.6% of the ^{17}O isotope (Yeda, Israel) were used. The observed transverse relaxation rate (R_2) were calculated from the signal width at half-height ($\Delta\nu_{1/2}$): $R_2^{obs} = \pi\times\Delta\nu_{1/2}$. Paramagnetic contributions to the observed transversal relaxation rate (R_{2p}) were calculated by subtracting from R_2^{obs} the diamagnetic contribution measured at each temperature value on pure water enriched with 2.6% ^{17}O isotope.

Acknowledgements

FVCK: The author would like to thank the Brazillian agency FAPESP (Proc. 2012/23169-8, 2015/16624-9 and 2018/16040-5) for the financial support. FA: The research was supported by the EU and co-financed by the European Regional Development Fund under the projects GINOP-2.3.2-15-2016-00008.

Conflicts of interest

There are no conflicts of interest to declare.

Keywords: Ligands • Lanthanides • Relaxation • Thermodynamic • Kinetics

[1] L. M. De León-Rodríguez, A. F. Martins, M. Pinho, N. Rofsky, A. D. Sherry, *J Magn Reson Imaging* **2015**, *42*, 545–565.

[2] C. S. Bonnet, P. H. Fries, S. Crouzy, P. Delangle, *J. Phys. Chem. B* **2010**, *114*, 8770–8781.

[3] P. Caravan, J. J. Ellison, T. J. McMurry, R. B. Lauffer, *Chem Rev* **1999**, *99*, 2293–2352.

[4] A. S. Merbach, L. Helm, É. Tóth, *The Chemistry of Contrast Agents in Medical Magnetic Resonance Imaging*, Wiley, **2013**.

[5] C. F. G. C. Geraldes, S. Laurent, *Cont. Med. & Mol. Imag.* **2009**, *4*, 1–23.

[6] S. Aime, M. Botta, M. Fasano, E. Terreno, *Chem. Soc. Rev.* **1998**, *27*, 19–29.

[7] S. Hajela, M. Botta, S. Giraudo, J. Xu, K. N. Raymond, S. Aime, *J. Am. Chem. Soc.* **2000**, *122*, 11228–11229.

[8] E. J. Werner, J. Kozhukh, M. Botta, E. G. Moore, S. Avedano, S. Aime, K. N. Raymond, *Inorg Chem* **2009**, *48*, 277–286.

[9] E. Gianolio, G. B. Giovenzana, D. Longo, I. Longo, I. Menegotto, S. Aime, *Chemistry – A European Journal* **2007**, *13*, 5785–5797.

[10] E. Gianolio, C. Cabella, S. Colombo Serra, G. Valbusa, F. Arena, A. Maiocchi, L. Miragoli, F. Tedoldi, F. Uggeri, M. Visigalli, P. Bardini, S. Aime, *J. Biol. Inorg. Chem.* **2014**, *19*, 715–26.

[11] I. Mamedov, J. Engelmann, O. Eschenko, M. Beyerlein, N. K. Logothetis, *Chem. Commun.* **2012**, *48*, 2755–2757.

[12] L. Manzoni, L. Belvisi, D. Arosio, M. P. Bartolomeo, A. Bianchi, C. Brioschi, F. Buonsanti, C. Cabella, C. Casagrande, M. Civera, M. De Matteo, L. Fugazza, L. Lattuada, F. Maisano, L. Miragoli, C. Neira, M. Pilkington-Miksa, C. Scolastico, *ChemMedChem* **2012**, *7*, 1084–93.

[13] E. Farkas, J. Nagel, B. P. Waldron, D. Parker, I. Tóth, E. Brücher, F. Rösch, Z. Baranyai, *Chemistry – A European Journal* **2017**, *23*, 10358–10371.

[14] B. P. Waldron, D. Parker, C. Burchardt, D. S. Yufit, M. Zimny, F. Roesch, *Chem Commun (Camb)* **2013**, *49*, 579–81.

[15] J.-P. Sinnes, J. Nagel, B. P. Waldron, T. Maina, B. A. Nock, R. K. Bergmann, M. Ullrich, J. Pietzsch, M. Bachmann, R. P. Baum, F. Rösch, *EJNMMI Research* **2019**, *9*, 48.

[16] J. Martinelli, G. Gugliotta, L. Tei, *Org. Lett.* **2012**, *14*, 716–719.

[17] S. Aime, L. Calabi, C. Cavallotti, E. Gianolio, G. B. Giovenzana, P. Losi, A. Maiocchi, G. Palmisano, M. Sisti, *Inorg. Chem.* **2004**, *43*, 7588–90.

[18] Z. Baranyai, F. Uggeri, G. B. Giovenzana, A. Benyei, E. Brucher, S. Aime, *Chem-Eur J* **2009**, *15*, 1696–1705.

[19] Z. Baranyai, F. Uggeri, A. Maiocchi, G. B. Giovenzana, C. Cavallotti, A. Takács, I. Tóth, I. Bányai, A. Bényei, E. Brucher, S. Aime, *Eur. J. Inorg. Chem.* **2013**, *2013*, 147–162.

[20] Z. Baranyai, D. D. Castelli, C. Platas-Iglesias, D. Esteban-Gomez, A. Bényei, L. Tei, M. Botta, *Inorg. Chem. Front.* **2020**, *7*, 795–803.

[21] A. Vagner, E. Gianolio, S. Aime, A. Maiocchi, I. Toth, Z. Baranyai, L. Tei, *Chem Commun (Camb)* **2016**, *52*, 11235–8.

[22] D. Delli Castelli, L. Tei, F. Carniato, S. Aime, M. Botta, *Chem Commun (Camb)* **2018**, *54*, 2004–2007.

[23] L. Barcza, K. Mihályi, *Zeitschrift für Physikalische Chemie* **1977**, *104*, 199–212.

[24] M. Botta, *European Journal of Inorganic Chemistry* **2000**, *2000*, 399–407.

[25] K. Micskei, L. Helm, E. Brucher, A. E. Merbach, *Inorganic Chemistry* **1993**, *32*, 3844–3850.

[26] T. J. Swift, R. E. Connick, *J. Chem. Phys.* **1962**, *37*, 307–320.

[27] a) L. R. Tear, C. Carrera, E. Gianolio and S. Aime, *Chem. – Eur. J.* **2020**, *26*, 6056-6063; b) D. Delli Castelli, M. C. Caligara, M. Botta, E. Terreno and S. Aime, *Inorg. Chem.* **2013**, *52*, 7130-7138; c) C. Platas-Iglesias, *Eur. J. Inorg. Chem.* **2012**, *2012*, 2023-2033; d) S. Aime, M. Botta, Z. Garda, B. E. Kucera, G. Tircso, V. G. Young and M. Woods, *Inorg. Chem.* **2011**, *50*, 7955-7965.

[28] T. J. Clough, L. Jiang, K.-L. Wong, N. J. Long, *Nature Comm.* **2019**, *10*, 1420–1433.

[29] J. Wahsner, E. M. Gale, A. Rodríguez-Rodríguez, P. Caravan, *Chem. Rev.* **2019**, *119*, 957–1057.

[30] E. Brücher, G. Tircsó, Z. Baranyai, Z. Kovács, A. D. Sherry, in *The Chemistry of Contrast Agents in Medical Magnetic Resonance Imaging* (Eds.: A.S. Merbach, L. Helm, E. Toth), John Wiley & Sons, Ltd, **2013**, pp. 157–208.

[31] P. M. May, P. W. Linder, D. R. Williams, *J Chem Soc Dalton* **1977**, 588–595.

[32] Z. Baranyai, Z. Palinkas, F. Uggeri, A. Maiocchi, S. Aime, E. Brucher, *Chem-Eur J* **2012**, *18*, 16426–16435.

[33] Z. Baranyai, E. Brucher, F. Uggeri, A. Maiocchi, I. Toth, M. Andrasi, A. Gaspar, L. Zekany, S. Aime, *Chem-Eur J* **2015**, *21*, 4789–4799.

[34] A. Barge, G. Cravotto, E. Gianolio, F. Fedeli, *Contrast Media & Molecular Imaging* **2006**, *1*, 184–188.

[35] H. M. Irving, M. G. Miles, L. D. Pettit, *Analytica Chimica Acta* **1967**, *38*, 475–488.

[36] L. Zékány, I. Nagypál, in *Computational Methods for the Determination of Formation Constants* (Ed.: D. J. Leget), Plenum Press, New York, **1985**, pp. 291–353.

10.1002/chem.202004479

WILEY-VCH

Entry for the Table of Contents

Layout 1:

FULL PAPER

The good properties of Gd(AAZTA) as MRI contrast agent are further improved by simply attaching a short *n*-alkyl function on the ligand's surface. The VT-T_2 measurements of the $^{17}OH_2$ resonance suggest the occurrence of two interconverting isomers in solution characterized by very different exchange rates of the coordinated water molecules.

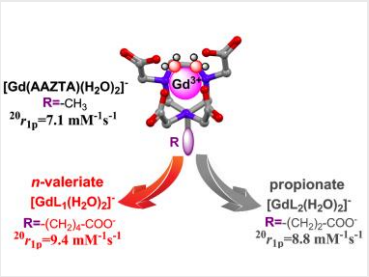

Flávio Vinicius Crizóstomo Kock, Attila Forgács, Nicol Guidolin, Rachele Stefania, Adrienn Vágner, Eliana Gianolio, Silvio Aime and Zsolt Baranyai**

Page No. – Page No.

[Gd(AAZTA)]$^-$ derivatives with *n*-alkyl acid side chains show improved properties for their application as MRI contrast agents